BUTTERWORTH HEINEMANN

Polymer Vol. 36 No. 1, pp. 87–91, 1995

0032-3861/95/$10.00+0.00

LCST-type phase behaviour and structure development during melt processing in a polycarbonate/poly(styrene-*co*-acrylonitrile) blend

Masami Okamoto* and Kiyoshi Shiomi
Toyobo Research Center, Toyobo Co. Ltd, Katata, Ohtsu, Shiga 520-02, Japan

and Takashi Inoue
Department of Organic and Polymeric Materials, Tokyo Institute of Technology, Ookayama, Meguro-ku, Tokyo 152, Japan
(Received 12 May 1994; revised 11 July 1994)

The lower critical solution temperature (*LCST*) type phase behaviour of a poly(styrene-*co*-acrylonitrile)/polycarbonate blend was verified by time-resolved light scattering analysis of the kinetics of both phase separation (above *LCST*) and phase dissolution (below *LCST*). The diffusion coefficient for separation was much larger than that of dissolution. The kinetic results provided a plausible scenario for the development of bicontinuous two-phase structure in the melt-processed blend as follows. When cold pellets of both polymers are heated to above the glass transition temperature (T_g) of the polymers in the extruder, dissolution starts. Even after attaining the spinodal temperature ($T_s = 223°C$) dissolution continues, since T_s can be elevated under shear to above the barrel temperature (260°C). The homogeneous melt is extruded and quenched quickly into water. When the single-phase blend is heated under high shear in an injection machine (at 290°C) and injected into a cold mould, spinodal decomposition proceeds until the melt is cooled down to T_s. The dissolution below T_s is negligible so that the bicontinuous structure attained via spinodal decomposition is frozen in the moulded blend by vitrification near T_g.

(Keywords: PC/SAN blends; melt processing; spinodal decomposition)

INTRODUCTION

Polycarbonate of bisphenol A (PC)/poly(styrene-*co*-acrylonitrile) (SAN) blend is an injection mouldable thermoplastic applied widely for automotive parts. Many experimental studies on PC/SAN blends have been devoted to the morphology–properties relationship. The miscibility was investigated at different levels of acrylonitrile (AN) in SAN by Keitz *et al.*[1]. Concerning the morphology development, some authors have claimed the importance of viscoelastic behaviour. Quintens *et al.*[2] reported that, in the injection moulded sheet of PC/SAN 60/40 blend, a bicontinuous structure is formed and the structure coarsens with increasing annealing time. The co-continuous structure may suggest that the structure formation proceeds via the spinodal decomposition.

In this paper, we undertake a kinetic analysis of the phase separation by time-resolved light scattering to justify the spinodal decomposition mechanism. On the basis of these results, we try to understand the morphology development in injection moulded PC/SAN blend.

* To whom correspondence should be addressed

EXPERIMENTAL

The blend in this study was prepared from commercial grades of PC copolymer (cPC) ($M_n = 2.4 \times 10^4$, glass transition temperature (T_g) = 192°C; APEC, Bayer Co.) and SAN (AN = 23 wt%, $M_n = 21 \times 10^4$, $T_g = 100°C$; Nippon Steel Co.). A 50/50 blend was made by melt extrusion, using a co-rotating twin-screw extruder (Ikegai Machinery Corp.; $\phi = 30$ mm, $L/D = 16$, barrel temperature = 260°C). The extruded melt was quickly quenched into water to freeze the structure in the melt and then chopped into pellets.

The pellets were pressed to a thin film (~20 μm thick) between two cover glasses at 220°C for 1 min. Immediately after the melt-pressing, the re-melted specimen was quickly transferred into the hot chamber on a light scattering apparatus and subjected to time-resolved light scattering measurement. The photometer is equipped with 46 photodiode array and facilitates the time-resolved measurement of scattering profile, angular dependence of scattered light intensity, with a time slice of 1/30 s (ref. 3). The radiation of a He–Ne laser of 632.8 nm wavelength was applied vertically to the film specimen and

the scattering profile was observed under V_v (parallel polarization) optical alignment.

The pellets were injection moulded to a sheet (30 mm × 120 mm × 2 mm) using an injection machine (Toshiba Machinery Corp., IS-100; barrel temperature = 290°C). The injection moulded specimen was mounted on an ultramicrotome (Ultracut N, Reichert-Jung) and microtomed to provide a new flat surface. The microtomed sample was stained with ruthenium tetroxide vapour for 1 day at room temperature. The morphology was observed under scanning electron microscopy (SEM) (Hitachi S-4500; 15 kV). Thus the SEM observation was carried out on the backscattered electrons from the microtomed and stained surface[4].

In order to analyse the cooling rate of the molten blend during injection moulding into a mould set at 95°C, the resin temperature was measured by embedding a thermocouple in the mould.

RESULTS AND DISCUSSION

Figure 1 is a SEM photograph of an injection moulded specimen of 50/50 cPC/SAN blend. A high level of connectivity of both phases can be seen and the phases are regularly spaced. Two-phase structure with unique periodicity and phase connectivity is one of the hallmarks of spinodal decomposition.

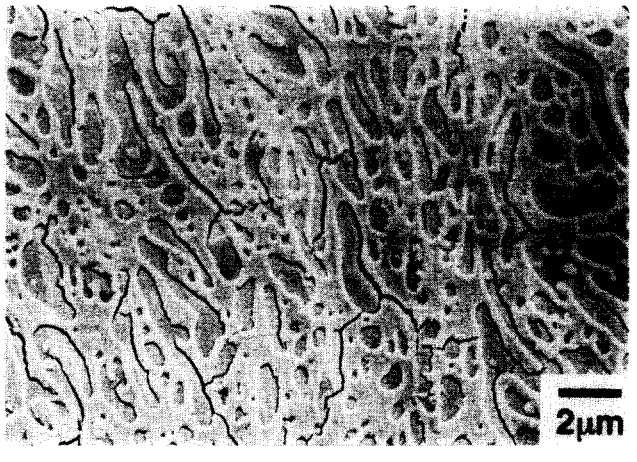

Figure 1 Scanning electron micrograph of injection moulded cPC/SAN 50/50 blend, using backscattering method for the microtomed and stained (RuO_4) sample

Figure 2 shows a typical example of the change in scattering profile with demixing time t at 260°C. Here, the scattered light intensity I is shown as a function of the magnitude of scattering vector q, defined by $q=(4\pi/\lambda')\sin(\theta/2)$, where λ' is the wavelength of light in the specimen and θ is the scattering angle. Note that, at $t=0$, the scattering intensity is very weak and the profile has hardly any q-dependence, suggesting that the extruded and re-melted blend is almost a homogeneous mixture. The homogeneous mixture starts to phase-separate by annealing at 260°C, as shown by the increase in the scattering intensity. The appearance of a scattering peak suggests that the demixing process is by the spinodal decomposition mechanism. To confirm this point, we analysed the early stage on the basis of the linearized Cahn–Hilliard theory[5].

In the early stage of spinodal decomposition, the scattering intensity is expected to increase exponentially with time:

$$I(q,t)=I(q,t=0)\exp[2R(q)t] \quad (1)$$

The amplification factor $R(q)$ is given by

$$R(q)=-Mq^2(\partial^2 f/\partial c^2+2kq^2) \quad (2)$$

where f is the local free energy of mixing, c is the concentration, k is the concentration-gradient energy coefficient and M is the mobility. According to equation (1), a plot of $\ln I$ *versus* t at a fixed q should yield a straight line of slope $2R(q)$. The linear regime is seen in the initial stage as shown in *Figure 3*, indicating that the initial stage can be described by the linearized theory. Linear results are also obtained at various q values.

Figure 4 shows a plot of $R(q)/q^2$ *versus* q^2. As expected from equation (2), the plot yields a good straight line for a large q regime, indicating again that the initial stage can be described within the framework of the linearized theory. From the plot one can estimate a series of characteristic parameters, q_m, q_c and D_{app}, which describe the dynamics of phase separation: q_c is the critical wavenumber of fluctuations that can grow, q_m is the most probable wavenumber of the fluctuation having the

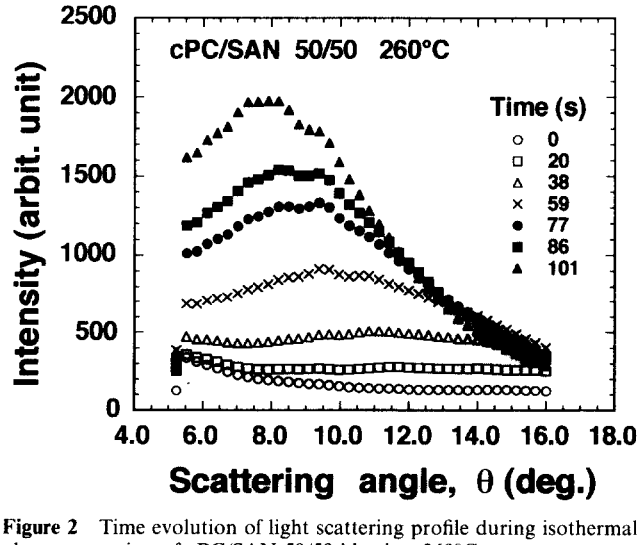

Figure 2 Time evolution of light scattering profile during isothermal phase separation of cPC/SAN 50/50 blend at 260°C

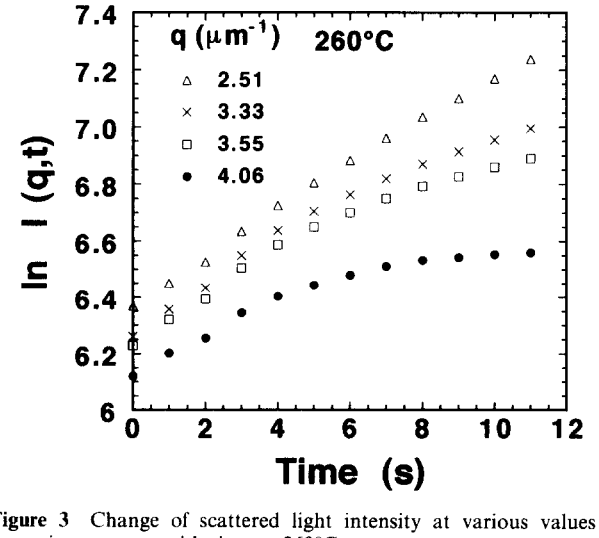

Figure 3 Change of scattered light intensity at various values of scattering vector q with time at 260°C

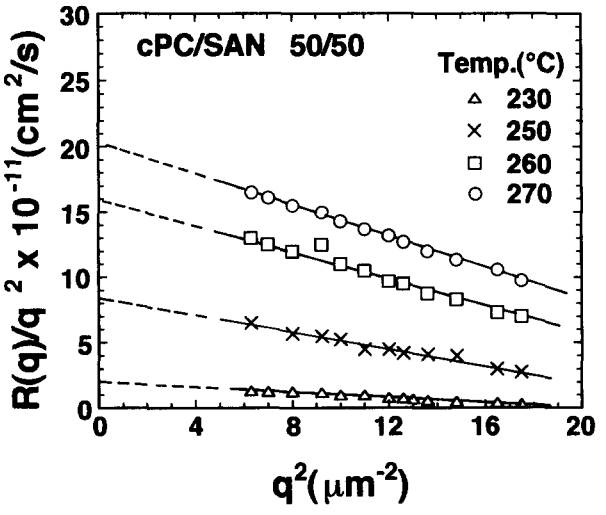

Figure 4 R(q)/q^2 *versus* q^2 plots at various temperatures

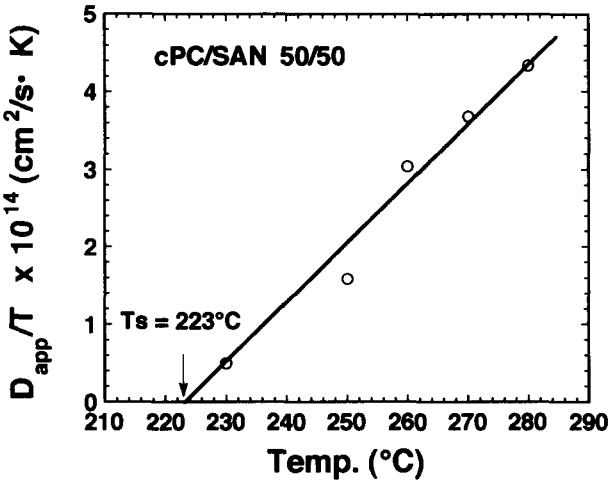

Figure 5 Temperature dependence of D_{app}

highest rate of growth and D_{app} is the apparent mutual diffusion coefficient. According to equation (2), q_c is given by the intercept on the q^2-axis, q_m is calculated from the relation $2q_m^2 = q_c^2$ and D_{app} is obtained from the intercept on the vertical axis. D_{app} is defined by

$$D_{app} = -M(\partial^2 f/\partial c^2) \tag{3}$$

and given by

$$D_{app} \propto D_c[|(\chi - \chi_s)|/\chi_s]^{\nu} \tag{4}$$

where D_c is the self-diffusion coefficient for translational diffusion, χ is the interaction parameter, χ_s is the interaction parameter at the spinodal temperature and ν is the critical exponent ($=1.0$) which will be discussed later in detail. Employing the relationship $D_c \propto T$ from the Stokes–Einstein equation and $[|(\chi - \chi_s)|/\chi_s] \propto |T - T_s|$ (T_s is the spinodal temperature), equation (4) leads to

$$D_{app} \propto T|T - T_s| \tag{5}$$

Figure 5 shows the temperature dependence of D_{app}. From the intercept on the T-axis at $D_{app}/T = 0$, one can estimate the T_s at which D_{app} is zero. The T_s thus obtained is 223°C. The results imply that the system has a lower critical solution temperature (*LCST*) type phase diagram.

Based on the above results, a scenario of the melt extrusion to yield homogeneous mixture may be given as follows (see *Figure 6*). Cold pellets of both polymers are fed into the extruder and are gradually heated. After the polymer temperature exceeds both T_gs, phase dissolution will start. Even after attaining T_s, the dissolution will be continued, since T_s can be elevated under shear[6,7]. Under the high shear rate in the extruder, T_s might be raised above the barrel temperature. Thus, the mixing could be done in a wide temperature window for dissolution to get a homogeneous mixture. The homogeneous state could be frozen by quenching quickly. Then, the homogeneous melt can be recovered by the re-melt at 220°C (below T_s).

In the late stage of phase separation, one can justify the self-similar growth of structure by scaling rules. In *Figure 7* is shown the universal curve in terms of dimensionless variables Q_m and τ defined by

$$Q_m = q_m/q_m(t=0) \tag{6}$$

$$\tau = D_{app} q_m^2 t \tag{7}$$

All the results for the time development of wavenumber Q_m are nicely superimposed to a master curve as predicted

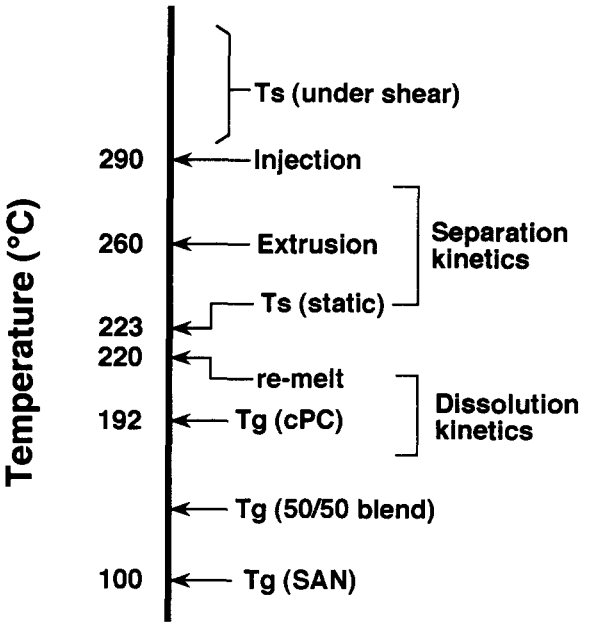

Figure 6 Transition and processing temperatures

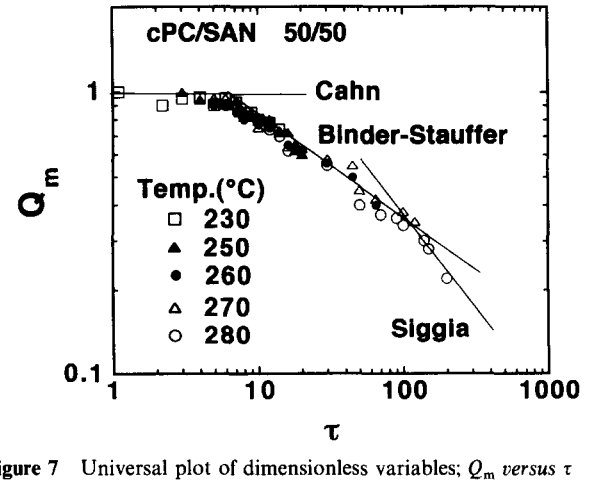

Figure 7 Universal plot of dimensionless variables; Q_m *versus* τ

theoretically by Binder and Stauffer[8] and Siggia[9], suggesting the self-similar growth mechanism.

To confirm further the *LCST* behaviour and investigate the dissolution kinetics below T_s, the phase-separated specimen at a late stage (at 250°C for 3 min) was subjected to temperature drops to temperatures below T_s (210–175°C) and annealed isothermally. As typically shown by *Figure 8*, the scattered intensity decreased with time of annealing, keeping the peak angle almost constant. This type of decay in the scattered intensity has already been discussed for the case of small angle X-ray scattering studies on the order–disorder transition in block copolymers by Hashimoto *et al.*[10] and in polymer blends by Takagi *et al.*[11]. The intensity decay in *Figure 8* corresponds to the phase dissolution of the bicontinuous structure, keeping the periodic distance constant, when the thermodynamic driving force for the phase separation is removed by the temperature drop to the single-phase region below T_s. The peak intensity I is plotted as a

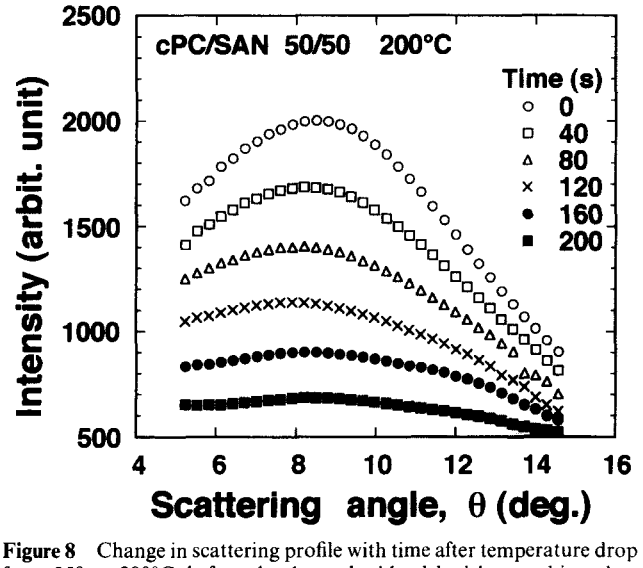

Figure 8 Change in scattering profile with time after temperature drop from 250 to 200°C; before the drop, the blend had been subjected to phase separation at 250°C for 3 min

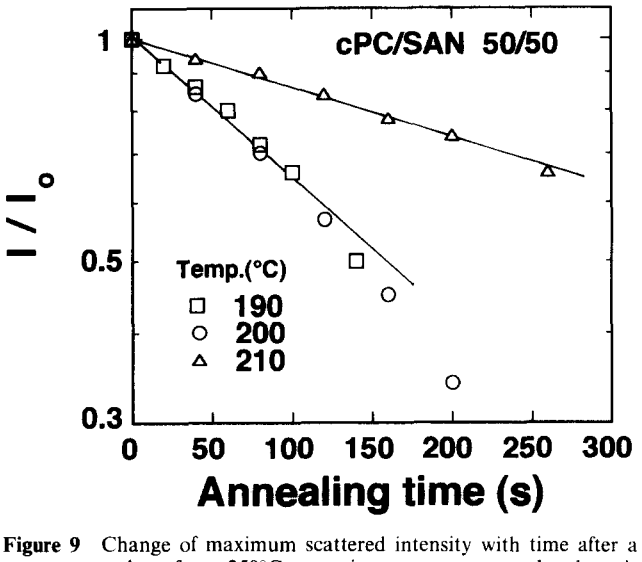

Figure 9 Change of maximum scattered intensity with time after a temperature drop from 250°C to various temperatures; the slope is related to D

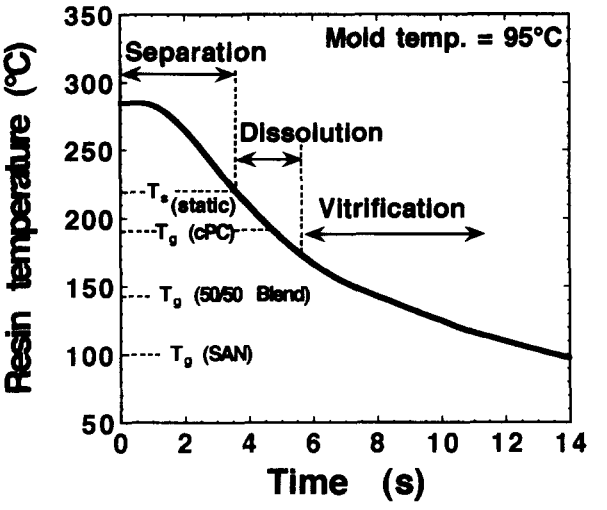

Figure 10 Apparent diffusion coefficients for separation and dissolution *versus* quench depth $|T-T_s|$

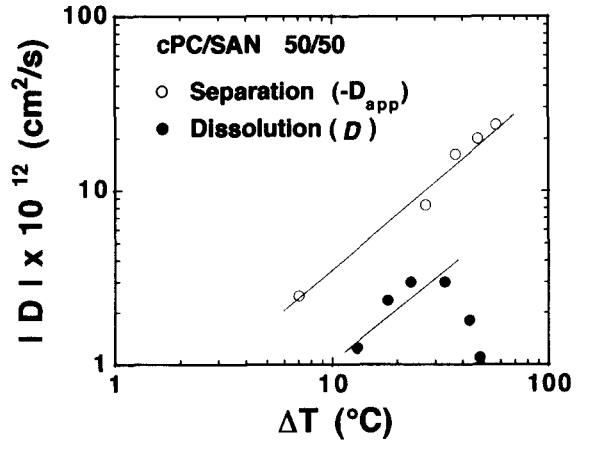

Figure 11 Change of resin temperature in mould with time after injection

function of time after the temperature drop in *Figure 9*. From the slope of the intensity decay, one can estimate the apparent diffusion constant D for the phase dissolution using:

$$\ln(I/I_0) = -2D[(4\pi/\lambda')\sin(\theta_m/2)]^2 t \quad (8)$$

where I_0 is the peak intensity at zero annealing time and θ_m is the scattering peak angle[12]. The linear decay of $\ln(I/I_0)$ *versus* time plots is seen in *Figure 9*. The D thus estimated increases from $\sim 10^{-13}$ to $\sim 10^{-12}\,cm^2\,s^{-1}$ with decreasing temperature from 210 to 190°C. At lower temperature, D decreases with decreasing temperature. The decrease in D may be caused by the decrease of chain mobility with approaching T_g.

The temperature dependence of D values both for dissolution and separation is given in *Figure 10* as a function of ΔT $(=|T-T_s|)$. Near T_s, the apparent diffusivity D_{app} for phase separation may be scaled as[13,14]

$$D_{app} = D_c \varepsilon^{\nu} \quad (9)$$

$$\varepsilon = [|T-T_s|]/T_s \quad (10)$$

where ν is the critical exponent, which has been found to be 1.0 for PS/poly(vinyl methyl ether) (PVME) blends by Snyder *et al.*[15]. In our system, a similar exponent ($\nu = 1$) is obtained, as predicted by the linearized theory of the Cahn–Hilliard model.

Figure 11 shows the change in resin temperature in the mould as a function of time after injection. Combining the results in *Figures 10* and *11*, one can see that (1) when the melt is out of the shear field in the mould, the spinodal temperature will drop to the static one ($T_s = 223°C$) and phase separation with large D will proceed until the melt is cooled down to T_g; (2) phase dissolution with small D will be negligible in a limited time at the cooling process; and then (3) the phase-separated structure via spinodal decomposition could be frozen by approaching the T_g of the demixed system (T_g of cPC-rich phase).

ACKNOWLEDGEMENTS

The authors express their appreciation to Dr Heinz-J. Fuellmann, Bayer Japan Ltd, for fruitful discussion and are also indebted to Mr Nobumasa Ishiai for supplying the co-polycarbonate, APEC HT series.

REFERENCES

1 Keitz, D. J., Barlow, W. and Paul, D. R. *J. Appl. Polym. Sci.* 1984, **29**, 3131
2 Quintens, D., Groeninckx, G., Guest, M. and Aerts, L. *Polym. Eng. Sci.* 1990, **22**, 1474
3 Suehiro, S. *Nikkei Electronics* 1986, No. 936, 213
4 Goizueta, G., Chiba, T. and Inoue, T. *Polymer* 1993, **34**, 253
5 Cahn, J. W. and Hilliard, J. E. *J. Chem. Phys.* 1958, **28**, 258
6 Wolf, B. A. *Macromolecules* 1984, **17**, 651
7 Hindawi, I., Higgins, J. S. and Weisis, R. A. *Macromolecules* 1990, **23**, 670
8 Binder, K. and Stauffer, D. *Phys. Rev. Lett.* 1973, **33**, 1006
9 Siggia, E. D. *Phys. Rev.* (*A*) 1979, **20**, 595
10 Hashimoto, T., Tsukahara, T. and Kawai, H. *Macromolecules* 1981, **14**, 708
11 Takagi, Y., Ougizawa, T. and Inoue, T. *Polymer* 1987, **28**, 103
12 Eichler, H., Salje, G. and Stahl, H. *J. Appl. Phys.* 1973, **44**, 5383
13 van Aartsen, J. J. *Eur. Polym. J.* 1970, **6**, 1105
14 Hashimoto, T., Kumaki, J. and Kawai, H. *Macromolecules* 1983, **16**, 641
15 Snyder, H. L., Meakin, P. and Reich, S. *Macromolecules* 1983, **16**, 757